New Geochemical Insights into the Petrogenesis of South Australian Kimberlites

Hayden Dalton[1], Andrea Giuliani[2], Angus Fitzpayne[2]

[1] *School of Geography, Earth and Atmospheric Sciences, University of Melbourne, Parkville 3010, Victoria, Australia (hayden.dalton@unimelb.edu.au)*

[2] *Institute for Geochemistry and Petrology, Department of Earth Sciences, ETH Zürich, Clausiusstrasse 25, CH-8092 Zürich, Switzerland (andrea.giuliani@erdw.ehtz.ch)*

Introduction

The occurrence of 'kimberlites' in South Australia has been documented since at least the 1970s (e.g., Colchester 1972; Scott-Smith, et al. 1984) following systematic exploration by De Beers, although alluvial diamonds had been already discovered by gold prospectors in the 19th century. Despite this history, and the subsequent discovery of over 200 occurrences of kimberlites and similar ultramafic rock types, relatively little is known about the petrogenesis and mantle source of these bodies.

Here, we present new petrographic and whole-rock geochemical and Sr-Nd-Hf isotopic data, including perovskite and calcite Sr isotopes, for Jurassic kimberlites (Cleve, Mount Hope and Pine Creek) and ultramafic lamprophyres (UMLs; Angaston, Terowie and Eurelia) from South Australia that have intruded through either the Late Archean to Mesoproterozoic Gawler Craton (Cleve and Mount Hope) or the Neoproterozoic to Cambrian Adelaide fold-belt (the remaining clusters).

Results and Discussion

Petrographically, the kimberlites and ultramafic lamprophyres are distinguished by a greater abundance of phlogopite and the presence of magmatic clinopyroxene in the latter. Major element compositions for these rocks vary widely (Fig. 1), possibly owing to a combination of magmatic differentiation, crustal contamination and post-emplacement alteration processes. For example, SiO_2 contents vary from as 12.2 wt.% to 58.1 wt.% for two samples from Terowie. The major element compositions of the kimberlites (Cleve, Mount Hope, Pine Creek) both overlap with, and extend beyond, the 'typical' compositions of global hypabyssal kimberlites. Excepting perhaps Terowie, the samples classified above as UMLs (Angaston and Eurelia) tend to have elevated K_2O, Al_2O_3 and Fe_2O_3, and lower MgO contents, consistent with their mineralogy being dominated by phlogopite $\pm$ clinopyroxene over olivine (Fig. 1). Relative to kimberlites, enrichments in these elements and Ti are also typical of UMLs globally. Incompatible element ratios (e.g., Ba/Nb, La/Nb, Th/U) show less variability and there is a strong overlap with the South Australian samples and compositions of global kimberlites, UMLs, and ocean island basalts.

Both the kimberlites and UMLs occupy a relatively narrow range in $^{87}Sr/^{86}Sr_{(i)}$ space (~0.704) based on in-situ perovskite data (Fig. 2), which are also consistent with perovskite Sr isotope values from Tappert, et al. (2019) for the same and/or related localities in the Adelaide Fold Belt. However, as is typical of these rocks, perovskite Sr isotope values diverge from data derived from whole-rock analyses ($^{87}Sr/^{86}Sr_{(i)} > 0.710$), which exhibit a strong positive correlation (not shown, $R^2 = 0.81$, $p = 0.000$) with bulk-rock SiO_2 contents, likely as a result of crustal contamination. It is notable that in some instances the carbonate within these samples can apparently faithfully record the magmatic $^{87}Sr/^{86}Sr_{(i)}$ composition, whilst in others these values record crustal contamination ($^{87}Sr/^{86}Sr_{(i)} > 0.715$), similar to what has been observed for kimberlites elsewhere (e.g., Castillo-Oliver, et al. 2018).
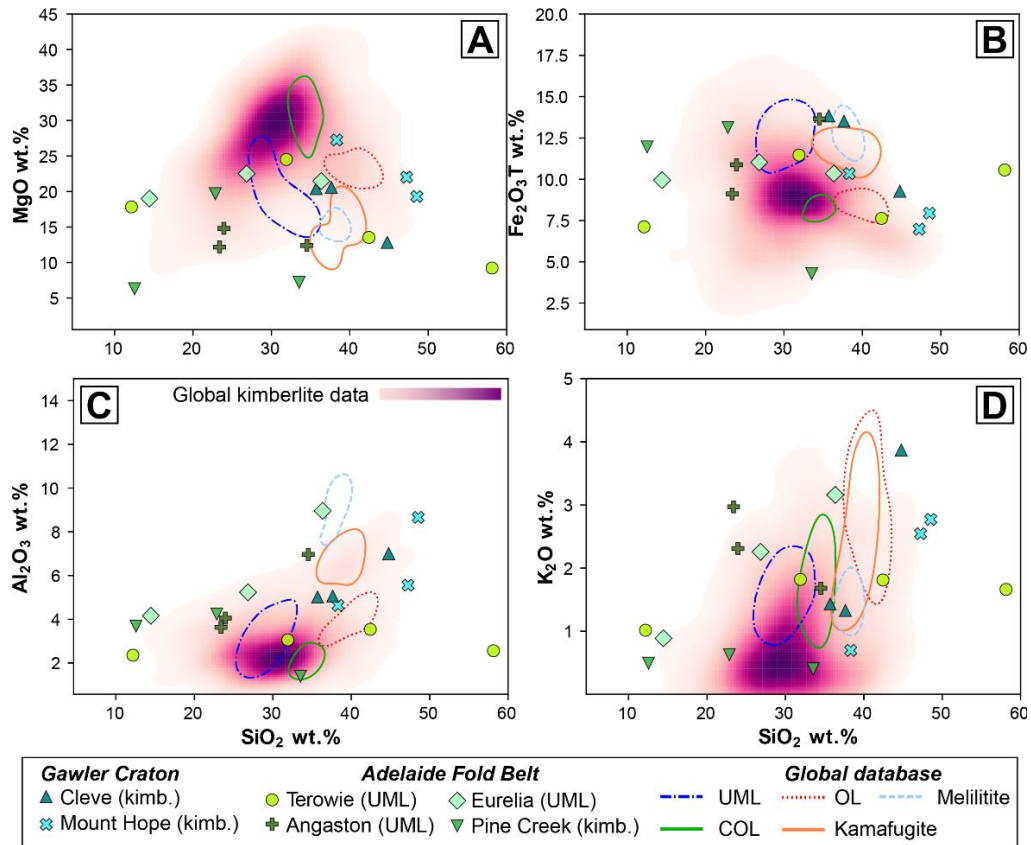
Figure 1. Major oxide co-variation charts for South Australian kimberlites and UMLS. Also plotted are global kimberlite data from Giuliani et al. (2024) using a gaussian kernel density estimation to highlight the most 'typical' compositions (using pyrolite; Williams, et al. 2020): SiO_2 vs a) MgO; b) Fe_2O_3; c) Al_2O_3; d) K_2O. Also plotted are compositional fields for ultramafic lamprophyres (UML), carbonate-rich olivine lamproites (COL), olivine lamproites (OL), kamafugites and melilitite (data from Giuliani et al., 2024). Each field represents the high-density area that contains 75% percent of values based on kernel density estimates for the data compiled.
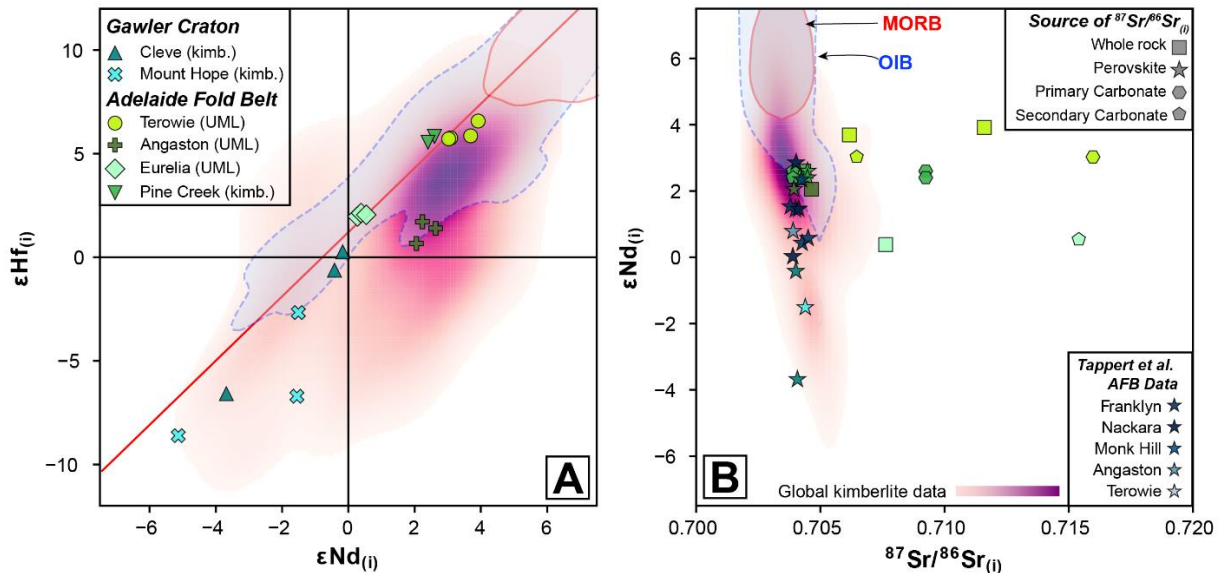

Figure 2. Radiogenic isotope co-variation charts for Australian kimberlites and UMLS. Also plotted are global kimberlite data from Giuliani, et al. (2024) and data for related Adelaide Fold Belt localities from Tappert et al. (2019): a) $\varepsilon Nd_{(i)}$ vs $\varepsilon Hf_{(i)}$; b) $^{87}Sr/^{86}Sr_{(i)}$ vs $\varepsilon Nd_{(i)}$.

In contrast to the near-invariant 'primary' (i.e., perovskite-derived) Sr isotopic compositions, Nd-Hf data reveals a possible spatiotemporal pattern in the source of kimberlites and UMLs from South Australia (Fig. 2, 3). The Cleve and Mount Hope kimberlites display geochemically-enriched Nd-Hf compositions that are somewhat atypical of kimberlites elsewhere, with strongly negative $\varepsilon Hf_{(i)}$ (down to -8) and $\varepsilon Nd_{(i)}$ (down to -4) values (Fig. 2). It is significant that these 'enriched' values are observed only in the two clusters of kimberlites that have intruded through the Gawler Craton, whereas the $\varepsilon Hf_{(i)}$ (+0.7 to +6.6) and $\varepsilon Nd_{(i)}$ (+0.3 to +3.9) values for the UMLs and kimberlites of the Adelaide Fold Belt reflect a relatively more geochemically-depleted mantle source.

Regarding the Adelaide Fold Belt, we observe that the younger intrusions record the more geochemically enriched source regions (i.e., Eurelia and Angaston) relative to the more depleted signatures observed in the oldest intrusions (i.e., Terowie and Pine Creek; Fig. 3). Overall, our results underscore a complex spatio-temporal pattern in the source of Jurassic diamondiferous magmas in South Australia.
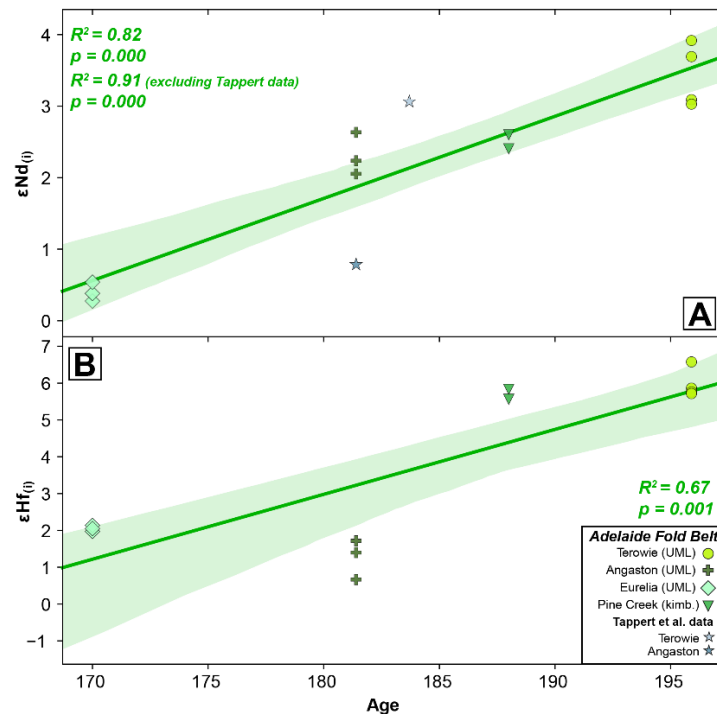

Figure 3. Temporal pattern in $\varepsilon Nd_{(i)}$ and $\varepsilon Hf_{(i)}$ compositions for kimberlites and UMLs from the Adelaide Fold Belt. Note the progression towards more "enriched" isotopic compositions for younger intrusions.

References

Castillo-Oliver M, Giuliani A, Griffin WL, O'Reilly SY (2018) Characterisation of primary and secondary carbonates in hypabyssal kimberlites: an integrated compositional and Sr-isotopic approach. Mineralogy and Petrology 112(2):555-567

Colchester DM (1972) A preliminary note on kimberlite occurrences in South Australia. Journal of the Geological Society of Australia 19(3):383-386

Giuliani A, Dalton H, Pearson DG (2024) Kimberlites: the deepest geochemical probes of Earth. In: Chauvel C (ed) The Treatise on Geochemistry, 3rd edition, Elsevier,

Scott-Smith BH, Danchin R, Harris J, Stracke K (1984) Kimberlites near Ororoo, South Australia. In: Kornprobst J (ed) Kimberlites I: Kimberlites and Related Rocks, vol 1. Elsevier, Amsterdam, pp 121-142

Tappert R, Foden J, Heaman L, Tappert MC, Zurevinski SE, Wills K (2019) The petrology of kimberlites from South Australia: Linking olivine macrocrystic and micaceous kimberlites. Journal of Volcanology and Geothermal Research 373:68-96

Williams MJ, Schoneveld L, Mao Y, Klump J, Gosses J, Dalton H, Bath A, Barnes S (2020) pyrolite: Python for geochemistry. The Journal of Open Source Software 5(50):2314